



The interplay of hydraulic failure and cell vitality explains tree capacity to recover from drought.

Marylou Mantova, Paulo Eduardo Menezes-Silva, Eric Badel, Hervé Cochard,
Jose Manuel Torres Ruiz

► To cite this version:

Marylou Mantova, Paulo Eduardo Menezes-Silva, Eric Badel, Hervé Cochard, Jose Manuel Torres Ruiz. The interplay of hydraulic failure and cell vitality explains tree capacity to recover from drought.. *Physiologia Plantarum*, In press, 172 (1), pp.247-257. 10.1111/ppl.13331 . hal-03109304

HAL Id: hal-03109304

<https://hal.inrae.fr/hal-03109304>

Submitted on 26 Apr 2021

HAL is a multi-disciplinary open access archive for the deposit and dissemination of scientific research documents, whether they are published or not. The documents may come from teaching and research institutions in France or abroad, or from public or private research centers.

L'archive ouverte pluridisciplinaire **HAL**, est destinée au dépôt et à la diffusion de documents scientifiques de niveau recherche, publiés ou non, émanant des établissements d'enseignement et de recherche français ou étrangers, des laboratoires publics ou privés.



Physiologia Plantarum

The interplay of hydraulic failure and cell vitality explains tree capacity to recover from drought

Journal:	<i>Physiologia Plantarum</i>
Manuscript ID	PPL-2020-00725.R1
Manuscript Type:	Regular manuscript - Ecophysiology, stress and adaptation
Date Submitted by the Author:	n/a
Complete List of Authors:	Mantova, Marylou; INRAE- University Clermont Auvergne Menezes Silva, Paulo; Instituto Federal de Educação Ciência e Tecnologia Goiano - Campus Rio Verde, Department of biology Badel, Eric; INRAE - University Clermont Auvergne Cochard, Hervé; INRA Centre Clermont-Ferrand-Theix-Lyon Torres-Ruiz, José M.; INRAE - University Clermont Auvergne, PIAF
Key Words:	cavitation, drought, tree mortality, cell death, Plant Hydraulics

1
2
3
4
5
6
7
8
9
10
11
12
13
14
15
16
17
18
19
20
21
22
23
24
25
26
27
28
29
30
31
32
33
34
35
36
37
38
39
40
41
42
43
44
45
46
47
48
49
50
51
52
53
54
55
56
57
58
59
60

The interplay of hydraulic failure and cell vitality explains tree capacity to recover from drought

Marylou Mantova¹, Paulo E. Menezes-Silva², Eric Badel¹, Hervé Cochard¹, José M. Torres-Ruiz^{1,*}

¹Université Clermont Auvergne, INRAE, PIAF, 63000 Clermont-Ferrand, France

²Laboratório de Fisiologia Vegetal, Instituto Federal de Educação, Ciência e Tecnologia Goiano, IF Goiano, 75901970 Rio Verde, Brasil

Correspondence

*Corresponding author,
e-mail : torresruizjm@gmail.com

Abstract

Global climatic models predict an increment in the frequency and intensity of drought events, which have important consequences on forest dieback. However, the mechanisms leading to tree mortality under drought conditions and the physiological thresholds for recovery are not totally understood yet. This study aimed to identify what are the key physiological traits that determine the tree capacity to recover from drought. Individuals of a conifer (*Pseudotsuga menziesii* M.) and an angiosperm (*Prunus lusitanica* L.) species were exposed to drought and their ability to recover after rehydration monitored. Results showed that the actual thresholds used for recovery from drought based on percentage loss of conductance (PLC) (i.e. 50% for conifers, 88% for angiosperms) do not provide accurate insights about the tree capacity for surviving extreme drought events. On the contrary, differences in stem relative water content (RWC_{Stem}) and the level of electrolytes leakage (EL) were directly related to the capacity of the trees to recover from drought. This was the case for the conifer species, *P. menziesii*, for which higher RWC_{Stem} and lower EL values were related to the recovery capacity. Even if results showed a similar trend for the angiosperm *P. lusitanica* as for the conifers, differences between the two traits were much more subtle and did not allow an accurate differentiation between trees able to recover and those that were not. RWC_{Stem} and EL could work as indicators of tree capacity to recover from drought for conifers but more studies are required to confirm this observation for angiosperms.

1
2
3
4
5
6
7
8
9
10
11
12
13
14
15
16
17
18
19
20
21
22
23
24
25
26
27
28
29
30
31
32
33
34
35
36
37
38
39
40
41
42
43
44
45
46
47
48
49
50
51
52
53
54
55
56
57
58
59
60

Introduction

Forests represent ca. 30% of the global continental surface (FAO 2006) and provide society with several ecosystem services such as timber production, watershed protection (Allen et al. 2010), hosting biodiversity (Trumbore et al. 2015), and carbon storage and its associated atmospheric feedbacks (Reichstein et al. 2013). Due to the ongoing climate changes and global warming (IPCC 2014), not only the frequency of heatwaves and drought events have increased in many areas worldwide but also their duration and intensity (Allen et al. 2010). A recent data synthesis has suggested that the majority of plant species converge to narrow hydraulic safety margins and thus are very susceptible to changes in rainfall patterns (Choat et al. 2018). Therefore, these higher frequencies and increased severity have exacerbated the occurrence of drought-induced tree mortality events (Keenan et al. 2013, Duan et al. 2014) and, consequently, forests dieback (Hosking and Hutcheson 1988, Lwanga 2003, Landmann and Dreyer 2006).

Although the reduction in water availability can affect virtually all processes associated with plant growth and development, drought-induced tree mortality events are commonly associated with two main processes: carbon starvation and xylem hydraulic failure (McDowell et al. 2008). Under prolonged mild drought conditions, trees partially close their stomata to reduce evapotranspiration and hence the risk of xylem hydraulic failure. However, this stomatal closure constrains CO₂ diffusion in leaves and can lead to an important depletion of the carbohydrate pools resulting in carbon starvation (Hogg and Hurdle 1997, Buckley 2005, McDowell et al. 2008, Berry et al. 2010, Creek et al. 2020). Even if carbon starvation and xylem hydraulic failure cannot be considered as mutually exclusive processes, recent studies have shown that xylem hydraulic failure is the main cause of tree mortality under severe drought (Urli et al. 2013, Salmon et al. 2015, Adams et al. 2017). Xylem hydraulic failure occurs when the tension in the continuous columns of water that connect the roots with the leaves through the xylem increases and, consequently, exacerbates the risk of cavitation (breakage of the water column) (Tyree and Zimmermann 2002). This process is widely amplified as soil dries or when the evaporative demand increases. Thus, under extreme drought conditions, as the percentage of cavitated conduits increases, the hydraulic conductance of the xylem decreases until the flow of water stops and provokes the desiccation of the plant tissues, cells death and, finally, the death of the tree (McDowell et al. 2008). This makes xylem vulnerability to cavitation one of the main physiological traits when evaluating drought-induced mortality.

Even if the vulnerability to cavitation has been widely evaluated for an important amount of species during the last decades (Delzon et al. 2010, Choat et al. 2012), the relationship between xylem hydraulic failure and tree mortality has not been properly evaluated yet. It is known that P_{50} and P_{88} (i.e. the xylem tension inducing 50 and 88% of loss of hydraulic conductance, respectively) are associated with the capacity of the trees to recover from drought (Brodribb et al. 2010, Delzon and Cochard 2014,

Sperry and Love 2015, Bolte et al. 2016), but the physiological causes of tree death under extreme drought events remain unclear. Therefore, due to a lack of physiological thresholds to properly define tree mortality both during or after a drought episode, P_{50} and P_{88} values, for conifers and angiosperms respectively (Brodribb and Cochard 2009; Urli et al. 2013), are currently used as proxies for mortality when e.g. modelling the trees' response to drought (Martin-StPaul et al. 2017). However, a recent study by Hammond et al. (2019) reported that the appropriateness of P_{50} as an indicator of mortality for conifers should be reconsidered as they defined a lethal threshold at 80% of loss of xylem hydraulic conductivity in loblolly pines (*Pinus taeda* L.). Also, it has recently been reported that branch diameter variations were revealing a point of no recovery in lavender species as plants were not able to recover from drought once their elastic water storage localized in the bark were depleted (Lamacque et al. 2020). These results have raised new questions about the role of xylem hydraulic failure in triggering tree mortality or the minimum hydraulic functioning required for allowing trees to survive and recover from drought.

The ability of the trees to recover after a drought event seems to be tightly related to their ability to grow new xylem (Brodribb et al. 2010) and this ability must be intrinsically linked to their capacity to maintain key living tissues alive in perennial organs, as the stem, that allow them to regrowth and resprout in favourable conditions. Considering the tenet that xylem hydraulic failure should provoke the complete desiccation of the cells and their consequent death leading to whole plant mortality (McDowell et al. 2008), a focus on plant water status and its consequences on cell vitality seems necessary to understand drought-induced mortality (Guadagno et al. 2017, Martinez-Vilalta et al. 2019). This, therefore, highlights the relevance of relative water content (RWC), a direct measure of the plant water status at cell level, as a potential candidate for assessing drought-induced tree mortality (Martinez-Vilalta et al. 2019, Trueba et al. 2019). In addition, and considering that many studies have evinced how low RWC values are linked to membrane dysfunction in plant cells (Wang et al. 2008, Chaturvedi et al. 2014), combining both traits, RWC and membrane dysfunction, would help define physiological thresholds for tree mortality.

The main objective of this study was to identify other physiological traits than the percentage loss of hydraulic conductance (PLC) that could work as an indicator of the tree capacity to recover from drought. For this, a set of plants of *Prunus lusitanica* L. and *Pseudotsuga menziesii* M., i.e. an angiosperm and a conifer species respectively, were exposed to severe drought conditions and allowed to dehydrate until the induction of important losses in hydraulic functioning. At this point, trees were re-watered to check for the capacity to recover from drought. During the dehydration and the recovery phases, we monitored embolism formation and changes in RWC at the stem and the leaf level. We also monitored changes in stem diameter to check whether trees were able to recover from drought after being re-watered, and assessed the vitality of the stem living tissues. Results also provided us with novel

information about the causative relationship between PLC and tree mortality and the level of PLC that prevent any recovery from drought in these two species.

Materials and methods

Plant material and experimental setup

The experiments were carried out in two species: one angiosperm, *Prunus lusitanica* L. and one conifer, *Pseudotsuga menziesii* M., a shrub and a tree respectively, selected for their contrasted PLC thresholds of drought-induced mortality (i.e. P_{88} and P_{50} respectively). For each species, eight young trees were grown under non-limiting water conditions in 5 and 9.2-L pots, respectively, at the INRAE-PIAF research station of Clermont-Ferrand, France (45°57'N, 3°14'E). *P. menziesii* individuals were four years old at the time of the experiment while the *P. lusitanica* were two years old. Two weeks before starting the experiment, all trees were moved to a controlled-environment glasshouse cell and kept under natural light and at a mean temperature of $17.7 \pm 0.2^\circ\text{C}$ (midday) and $10.9 \pm 0.1^\circ\text{C}$ (night). During this period, trees were kept well-irrigated (field capacity) by a drip irrigation system controlled by an electronic timer. After the two weeks of acclimation, a sub-set of trees for each species (from four to six individuals) was exposed to progressive dehydration by withholding the irrigation. In order to determine the critical PLC for recovery and because Hammond et al. (2019) reported that conifers were able to recover even beyond P_{50} , trees were re-watered to field capacity once reaching water potential values corresponding to significant losses in hydraulic functioning according to their vulnerabilities to cavitation (i.e. PLC > 50% for conifers and PLC > 90% for angiosperms). They were then kept well-irrigated in order to check for recovery from drought.

Vulnerability curves to cavitation

Prior to the experiment, the vulnerability to cavitation for the two target species was determined to define when trees should be re-watered according to their PLC level. Thus, two different techniques (i.e. one technique per species), reported as highly comparable by Brodribb et al. (2017), were used according to the xylem characteristics of each species. Thus, for *P. lusitanica*, xylem vulnerability to cavitation was determined by using the recently developed optical method (Brodribb et al. 2017) to avoid possible biased results related with the open-vessel artefact (Torres-Ruiz et al. 2014, 2015, Choat et al. 2016). Indeed, the use of the Cavitrone method in this species was not possible due to the length of the xylem conduits that were longer than the diameter of the rotor available (Sergent et al. 2020). For *P. menziesii*, vulnerability curves were constructed by using the Cavitrone technique (Cochard 2002) which is highly reliable when used to measure species with short conduits such as conifers (Cochard et al. 2013, Torres-Ruiz et al. 2017). The use of the optical method was not possible for *P. menziesii* because the conduits at the stem level are so short that the cavitation events are not always detectable.

Briefly, for *P. lusitanica*, the entire plant was let to dehydrate under lab conditions while a clamp equipped with a camera was installed in the stem of four trees after removing the bark carefully with a razor blade to expose undamaged xylem. To avoid the over desiccation of the exposed xylem area during the 6.51 ± 0.52 days of dehydration, we applied a thin coat of silicone grease. The camera then captured images every five min during the dehydration process while changes in stem water potential (Ψ_{stem} , MPa) were continuously monitored using a psychrometer (PSY1, ICT international, Armidale, Australia) installed centrally on the main stem of each plant. The Peltier cooling time was adjusted from 10 s (when the plant was well hydrated) to a maximum of 20 s (as the plant dehydrated) to ensure that sufficient water was condensed onto the thermocouple and then evaporated to produce a stable reading of the wet-bulb depression temperature. To ensure the accuracy of the measurements obtained with the psychrometer, regular Ψ_{stem} measurements were carried using a Scholander-type pressure chamber (PMS, Corvallis) in fully developed and healthy leaves previously bagged for at least one hour to prevent transpiration and promote equilibrium with the plant axis (Fig. S1). Image sequences were then analysed manually according to Brodribb et al. (2016, 2017). The percentage of embolised pixels for each image was calculated as the amount of embolised pixels cumulated and the total embolised area of the scanned area. The vulnerability curve was obtained by plotting Ψ_{stem} against cumulative embolisms (% of total).

For *P. menziesii*, xylem vulnerability to cavitation was assessed with the Cavitron technique (Cochard 2002) which uses centrifugal force to increase the water tension in a xylem segment while measuring the decrease in its hydraulic conductance. Thus, five 0.45m-long stem samples from five different well-hydrated trees (i.e. one sample per tree), were debarked to prevent resin contamination and recut under water with a razor blade to a standard length of 0.27m. For constructing the vulnerability curves, the maximum sample conductivity (K_{max}) was measured at low speed and relatively high xylem pressure (-0.75 MPa). The xylem pressure was then decreased stepwise by increasing the rotational velocity and the conductivity (K) measured at each pressure step. Each pressure was applied on the sample for two minutes. Sample loss of conductivity (PLC, %) was computed at each pressure as follows:

$$PLC = 100 * \left(1 - \frac{K}{K_{\text{max}}}\right) \quad (1)$$

The resulting curves were fitted according to Pammenter and Vander Willigen equation (1998) and using the R 'fitPLC' package:

$$PLC \text{ or Cumulative embolism} = \frac{100}{(1 + e^{(a/25(P - P_{50})})} \quad (2)$$

where a is the slope of the curve at the inflexion point, P indicates the xylem water potential for the optical method (*P. lusitanica*) or the target pressure reached with the Cavitron (*P. menziesii*), and P_{50} is

the Ψ_{stem} or pressure value at which 50% of the xylem cavitation events had been observed or at which 50% loss of conductivity occurred.

Physiological traits

During the progressive dehydration imposed to each subset of plants, Ψ_{stem} was continuously assessed by using psychrometers (PSY1, ICT international). Thus, one psychrometer per plant in a total of four plants per species was installed at the stem level and covered with aluminium foil to prevent their direct exposure to the sunlight and minimize any effect of external temperature variations (Vandeghechuchte et al. 2014). Psychrometers recorded the Ψ_{stem} every 30 min. To check the accuracy of the psychrometers, regular Ψ_{stem} measurements were carried using a Scholander-type pressure chamber (PMS, Corvallis) in two fully developed and healthy leaves per plant, previously bagged for at least one hour to prevent transpiration and promote equilibrium with the plant axis (Fig. S1).

Stem diameter variations were monitored continuously by Linear Variable Differential Transformer (LVDT) sensors (one LVDT per plant in eight plants per species) installed before withholding irrigation. The sensor was applied on the stem with glue and was connected to a data logger (Model CR1000, Campbell Scientific LTD) to collect the stem diameter variations (in μm) every 10 min. By evaluating the dynamics of stem diameter during the dehydration and recovery phases of the experiment, we were able to evaluate the capacity of the trees to recover from drought (Lamacque et al. 2020).

The RWC was measured at stem (RWC_{Stem}) and leaf level (RWC_{Leaf}) in all trees before withholding irrigation (Control) and right before re-watering. RWC_{Stem} and RWC_{Leaf} were calculated according to Barrs and Weatherley (1962):

$$\text{RWC} = \frac{(FW - DW)}{(TW - DW)} (3),$$

where FW is the fresh weight measured immediately after sampling; TW is the turgid weight measured after immersing the stem in distilled water for 24 h (for RWC_{Stem}) or after soaking the leaf petiole for 24 h in distilled water (for RWC_{Leaf}); and DW is the dry weight of the samples after 24 h of drying in an oven at 72°C. All measurements were done using a precision scale (METTLER AE 260, DeltaRange®) and were performed on three healthy leaves or one to three small stem sections per plant (depending on plant material).

Once the trees reached water potentials corresponding to a PLC of ca. 88% for *P. lusitanica* and 50% for *P. menziesii* according to the vulnerability curves, the PLC was assessed in stems using two different, but comparable, techniques (Cochard 1992, Torres-Ruiz et al. 2014, Choat et al. 2016). For *P. lusitanica*, PLC was determined gravimetrically using a xylem embolism meter (XYL'EM, Bronkhorst). For *P. menziesii*, as it was impossible to restore the maximal conductance (K_{max}) due to the permanent

aspiration of the pit membrane against the cell walls (Cochard et al. 2013), the PLC was assessed by direct observation using X-Ray microtomography (Micro-CT, Nanotom 180 XS; GE) at the PIAF laboratory (INRAE) (Cochard et al. 2015). For both techniques, samples were cut progressively underwater to prevent artefactual increases in the amount of embolism in the samples (Torres-Ruiz et al. 2015).

For the XYL'EM, the PLC was evaluated in three stems (sample length ca. 30mm) per individual in eight individuals per species. The initial K (K_i) of each segment was determined using a filtered (0.22 μ m) 10 mm KCl and 1 mm CaCl₂ perfusion solution made with distilled water (Cochard et al. 2009), and applying a pressure head of 8.5 kPa until a steady-state K_i was attained. In order to determine the maximal conductance (K_{max}), samples from *P. lusitanica* were flushed with water at high pressure (200 kPa) for 20 minutes to remove all the embolism. PLC was then calculated using the following equation:

$$PLC = 100 * \left(1 - \frac{K_i}{K_{max}}\right) \quad (4)$$

For Micro-CT, one or two samples per plant were collected, as described for the gravimetric K measurements, and immediately immersed in liquid paraffin wax to prevent dehydration during the scanning. For each 21-min scan, 1000 images were recorded during the 360° rotation of the sample. The X-ray setup was fixed at 70kV and 240 μ A. At the end of the experiment, samples were cut 3mm above the scanned cross-section, injected with air (0.1MPa) and re-scanned to visualize all the conduits filled with air. The amount of PLC was computed by determining the ratio between the amount of cavitated conduits in the samples before and after cutting the sample.

Cell vitality

Cell vitality was assessed using two different methods: the electrolytes leakage test (EL) (Zhang and Willison 1987, Sutinen et al. 1992) and a fluorescein diacetate (FDA) staining process (Widholm 1972). Cell vitality was assessed in both control and drying trees right before rewatering the latter ones. For EL, one to three stem samples per plant (depending on plant material availability) were cut into ten 2-mm thick slices and immersed in test tubes containing 15mL of pure water. Test tubes were shaken at 60 shakes per min during 24h at 5°C to stop enzyme activity. Water conductivity of the effusate (C1) was then measured at room temperature using a conductimeter (3310 SET1, Tetracon® 325, WTW, Weilheim, Germany). Then, all the living cells were killed by autoclaving the samples at 121°C for 30 min (King and Ludford 1983), cooled down at room temperature (22°C approx.) for 60 min and the effusate maximal conductivity (C2) measured. The lysis percentage (EL) was then determined as:

$$EL = \frac{C1}{C2} * 100 \quad (5)$$

To stain the cytoplasm of stem living cells and quantify the amount of living cells and their location for each individual, FDA (F7378-10G, SIGMA-ALDRICH) was used. For this, two or three 60 µm-thick stem cross-sections were obtained with a microtome (Leica RM2165) and stained for 20 min in a 1% FDA solution (Widholm 1972). Cross-sections were observed using an inverted fluorescence microscope (Axio Observer Z1, ZEISS; Bright light or YFP filter) within the next hour after staining. An entire cross-section image was obtained by joining images with the same magnification taken from all the cross-section of the sample for both bright light and fluorescence observations. The percentage of bark living cells (BLC) for each cross-section was calculated as follow:

$$BLC = \frac{FA}{BA} * 100 \text{ (6)}$$

Where FA is the total fluorescent area of the sample and BA is the bark area determined using Fiji software (Schindelin et al. 2012).

Statistical analyses

Statistical analyses consisted of paired *t*-test (after testing for normality and homogeneity of variances) and Wilcoxon test (for non-normal distribution) and were performed using R programs to compare the set before the drought event (Control) and before re-watering. All tests were performed using a level of significance $\alpha = 0.05$.

Results

Capacity of recovery from drought

Vulnerability curves reported P_{50} -values of -6.07 and -3.73MPa for *P. lusitanica* and *P. menziesii*, respectively (Fig. 1). *P. lusitanica* individuals were thus rehydrated once they reached water potential values of ca. -9.0 to -10.0MPa i.e. above its P_{88} of -8.94MPa. *P. menziesii* were rehydrated once showing water potential of ca. -7.0 to -10.0 MPa (P_{88} = -5.34MPa).

In control conditions, the mean levels of PLC in the stem for *P. lusitanica* and *P. menziesii* were 6.9 (± 3.5 SE) and 7.40 (± 2.8 SE) respectively (Fig. 2). Right before applying the recovery irrigation, the mean PLC for *P. lusitanica* and *P. menziesii* were 94.4 (± 1.98 SE) and 79.5 (± 3.7 SE) respectively (Table S1) i.e. above the current point for xylem hydraulic failure for angiosperms (i.e. P_{88}) and conifers (i.e. P_{50}).

Stems showed a noticeable shrinkage for both species during the time-course of the dehydration for all individuals (Fig. 3). After rewatering, two *P. lusitanica* individuals that reached a mean PLC of 90.3 (± 8.3 SE) (Fig. 2A) showed an increase in stem diameter immediately after being re-hydrated and were considered as recovered trees (Fig. 3A). On the contrary, the six individuals that reached PLC of 95.8 (± 1.1 SE) showed a continuous decrease in stem diameter after the rehydration and were considered

as dead trees (Fig. 3C). For *P. menziesii*, only one individual that reached a Ψ_{stem} value of -7.48MPa and a PLC level of 67.9 (Fig. 2B) was able to recover in terms of trunk diameter after rewatering (Fig. 3B). All the other individuals continued to show a decrease in stem diameter during the re-watering phase after reaching a mean Ψ_{stem} value of -8.7MPa (± 0.5 SE) (Fig. 3D) and a mean PLC of 81.1 (± 3.8 SE) (Fig. 2B).

For both species, individuals that were able to recover from drought showed an increase in Ψ_{stem} concomitantly to the increase in stem diameter (Fig. 3A, B) while no recovery in Ψ_{stem} was noticed in trees considered as dead (Fig. 3C and Fig. 3D).

A significant decrease in RWC_{Stem} was observed for both species during dehydration as PLC increases (Fig. 4A and Fig. 4B; Table S2). In control *P. lusitanica* trees, RWC_{Stem} was of 92.3% (± 0.8 SE) whereas it dropped for those exposed to drought to 58.5% (± 1.5 SE) for recovered individuals and to 54.7% (± 3.6 SE) for dead individuals before re-watering. Differences in RWC_{Stem} , however, were not significant when comparing recovered and dead individuals. Similar results were observed for *P. menziesii*, with a significant decrease in RWC_{Stem} noticed for both recovered and dead individuals from drought. Thus, RWC_{Stem} decreased from 83.4% (± 1.1 SE) for control trees to 49.8% for recovered and 36.9% (± 1.9 SE) for dead trees.

Similar to RWC_{Stem} , RWC_{Leaf} was significantly impacted in both species during dehydration (Fig. 4C, D; Table S2). For *P. lusitanica*, RWC_{Leaf} decreased from 94.8 % (± 0.5 SE) (Control) to 56.9% (± 4.1 SE) in plants that recovered from drought and to 59.3 % (± 4.8 SE) in those that did not recover. For *P. menziesii*, RWC_{Leaf} went from 92.4 % (± 2.0 SE) (Control) to 53.5 % in recovered trees or 51.5 % (± 4.7 SE) in dead trees. Differences in RWC_{Leaf} were not significant for any of the two species when comparing recovered and dead individuals.

Tissue vitality

For *P. lusitanica*, all trees showed higher EL values than control ones before re-watering (Fig. 4E and Fig. 4F, Table S2) (Control: 29.9% ± 1.3 SE; Recovered: 47.12% ± 7.12 SE; Dead: 57.2% ± 6.7 SE). However, no differences were noticed when comparing recovered and dead individuals before re-watering (Recovered: 47.1% ± 7.1 SE; Dead: 57.2% ± 6.7 SE). For, *P. menziesii*, only the trees that did not recover showed higher EL values compared to control (Control: 50.6% ± 2.2 SE; Dead: 78.8% ± 2.2 SE). No differences in EL were observed between the recovered individual and control ones (Control: 50.6% ± 2.2 SE; Recovered: 50.8%). The recovered individual tends to show lower EL values than the dead ones (Recovered: 50.8%; Dead: 78.8% ± 1.2 SE).

In control trees and for both species, the FDA staining showed that living cells were mostly located at the outer bark and phloem level (Fig. 5). Before re-watering, the amount of living cells in *P. lusitanica* decreased noticeably in dead trees (Fig. 6A; Table S3) (Control: 23.0% ± 4.4 SE; Dead: 3.0%

±1.4 SE) but not in trees that recovered (Control: 23.0% ±2.4 SE; Recovered: 15.3%±10.4 SE). For *P. menziesii*, the amount of living cells decreased in trees that did not recover (Control: 10.2% ±2.1 SE; Dead: 0.8% ±0.6 SE) while no noticeable decrease was encountered in trees that recovered (Control: 10.2% ±2.2 SE; R: 7.2%) (Fig. 6B; Table S3).

Discussion

Our results provide strong evidence that even when presenting high levels of hydraulic dysfunction, trees were able to recover from an extreme drought event after being re-watered. Indeed, *P. lusitanica* individuals that showed PLC values of 98.6%, i.e. well above the suggested threshold for recovery and point of death for angiosperms (P_{88} , Barigah et al. 2013; Urli et al. 2013), recovered from drought according to their stem diameter dynamic (i.e. showed an increase in stem diameter immediately after re-watering) and even flushed new leaves after being re-watered at field capacity (Fig. S2). Similarly, *P. menziesii* individuals with PLC values of 67.9%, i.e. above the threshold for recovery for conifers (P_{50} , Brodribb and Cochard 2009), were also able to recover once re-watered. These results, therefore, demonstrate how trees are able to recover from drought even when their PLC levels reach higher values than those considered as threshold for recovery for angiosperms and conifers (i.e. P_{88} and P_{50} , respectively). These results agree with those provided for loblolly pine (*Pinus taeda* L.) by Hammond et al. (2019) which reported a higher chance for trees to die than to survive once reaching PLC levels of 80, i.e. much higher than the P_{50} threshold commonly reported for conifers. In our study, however, no recovery was observed for *P. menziesii* when PLC reached values above 68%, which raises questions on how lethal PLC thresholds vary among tree species. For angiosperms, our results also agree with the ones provided for *Pistacia lentiscus* L. by Vilagrosa et al. (2003) that show how drought-induced mortality only occur in plants that reached PLC values of almost 100%. When taken together, all these results highlight the importance of revising the actual recovery and point of death thresholds suggested for angiosperms and conifers. More importantly, these results show that plant mortality occurs when the losses in xylem conductance are important (e.g. >90% of xylem hydraulic dysfunction), suggesting that PLC is not the sole triggering mechanism of plant death under drought conditions.

Unfortunately, any critical thresholds for most of the physiological traits monitored during our experiment were identified as a potential proxy for drought-induced mortality. Thus, it was not possible to evince a clear causal link between stem hydraulic failure and plant mortality since trees that were not able to recover from drought did not consistently show higher PLC values than those that survived. However, two interesting trends emerged from the RWC_{Stem} and EL results for *P. menziesii*. On one hand, trees recovering from drought tend to show higher RWC_{Stem} than dead ones before re-watering and, on the other hand, trees that recovered tend to show lower EL values than the dead ones. These results agree with Martinez-Vilalta et al. (2019) and highlight the importance of plant water content as a potential indicator of mortality risk. However, this was not the case for *P. lusitanica* since similar

RWC_{Stem} values were observed in both trees that were able to recover from drought and those that were not. This raises the possibility of using RWC_{Stem} as a proxy for mortality across species, although more confirmatory studies should be carried out especially in angiosperms. At leaf level, RWC_{Leaf} at turgor loss point is relatively high and constant between species (Bartlett et al. 2012), which potentially could make it a useful trait for identifying survival events since noticeable changes in RWC_{Leaf} would occur at high dehydration level preceding death (Martinez-Vilalta et al. 2019). However, no differences in RWC_{Leaf} were detected in our study between recovering and dead trees before re-watering for any of the two species evaluated probably because, at those levels of water stress, leaves were already hydraulically disconnected from the stems in all the individuals. This would favour a faster dehydration of the leaves in comparison with the stems and, therefore, may partially explain the similarly low values for RWC_{Leaf}. Therefore, rather than just focusing only on the plant water status, a deeper study on water relocation in trees during drought (Körner 2019) would be required for identifying potential proxies for drought-induced mortality. In fact, a crucial question now is to evaluate if the relocation of water from plant reserves would be enough for keeping key tree tissues hydrated during drought and, therefore, enhancing plant probability of survival after re-watering (Holbrook 1995).

Regarding cell integrity, recovering trees from drought tend to present lower cell damages than the dead trees before re-watering. *P. menziesii* recovering trees showed seemingly no changes in their percentage of EL even after the drought event. Dead trees, on the contrary, consistently showed higher EL values before re-watering than control trees able to recover in agreement with the results reported by Vilagrosa et al. (2010) for *P. lentiscus*. Even if *P. lusitanica* dead and recovering trees did not show any differences in EL, recovering trees were able to resprout and flush new leaves when the stress was alleviated (Fig. S2). As higher EL values are the consequences of membrane failure and are associated with cell death (Vilagrosa et al. 2010, Guadagno et al. 2017), these observations suggest that the fatal failure at the cellular scale does not occur homogeneously within the stem and this, as shown by Thomas (2013) and Klimešová et al. (2015), allow the resprouting of the plant if the stress is relieved. Therefore, according to our results, the membrane integrity could emerge as a proxy for lack of recovery capacity in conifers since the cell vitality in some of the living tissues at the stem level seems to have a relevant role in drought-induced mortality. However, the link between membrane failure and the loss in stem hydraulic functioning is still unresolved. Indeed, it is still unclear whether the extreme dehydration leads to membrane failure through physical (i.e. cell cavitation, Sakes et al. 2016), collapse and cytorrhysis (Taiz and Zeiger 2006) or only biochemical processes (Suzuki et al. 2012, Wang et al. 2013, Petrov et al. 2015).

The presence of living cells in stems at the inner bark level was not always related to the survival of the trees after re-watering (i.e. increase in stem diameter). This was the case for *P. lusitanica* where trees showing similar amounts of living cells, differed in their capacity to recover from drought. The presence of living cells in dead trees could be explained by the fact that, under drought conditions, trees

can rely on their own water reserves (Epila et al. 2017) which could temporally maintain the metabolism of the cell despite being hydraulically disconnected from the roots. However, once the water reserves are depleted, living tissues would ultimately dry and cells would dehydrate and die. Therefore, not only the presence of living cells is required for allowing the plant to recover from drought but also their hydraulic connection with the other plant tissues and organs upstream. Thus, even at stem PLC values near to 100% for angiosperms or well above 50% for conifers, a minimal hydraulic connection between the soil and the living tissues could be enough to recover from drought if plants have access to water. More studies focused on the link between xylem hydraulic functioning, plant capacitance and cell mortality are therefore required to identify what the thresholds for tree survival to drought are.

Conclusion

By combining a living-cell staining process with LVDT sensors and PLC measurements, this study showed that the common thresholds for recovery and point of death considered until now, i.e P_{50} for conifers and P_{88} for angiosperms, are not accurate enough for assessing and predicting drought-induced tree mortality. Indeed, our results showed that trees with PLC levels of 98.6% for *P. lusitanica* (angiosperm) and 67.9% for *P. menziesii* (conifer) were still able to recover from drought once re-watered. Thus, even if the link between a high level of stem PLC and tree mortality is clear, there is an urgent need in defining new physiological thresholds for predicting tree mortality with mechanistic models. For conifers, higher RWC_{Stem} and lower EL values were related to a higher capacity to survive drought. However, this was not the case for angiosperms for which no physiological traits were identified as a potential proxy for the capacity of plant to recover although a similar pattern as to the one observed for the conifer species was identified.

Author contributions

MM and JMTR conceived and designed the experiment. MM and PEMS were responsible for running the measurements and carried out the data analysis. EB supervised the setting up of the micro-CT scans. MM, PEMS, HC and JMTR interpreted the results. MM wrote the first manuscript draft. JMTR, PEMS, HC and EB assisted substantially with manuscript development.

Acknowledgement

The authors thank Pierre Conchon and Julien Cartailier for their technical assistance, and the PIAF Research Unit staff for their support during this experiment. This research was funded by the project ANR-18-CE20-0005 *Hydrauleaks*.

Data availability statement

The data are not publicly available due to privacy restrictions.

403

For Peer Review

1
2
3
4
5
6
7
8
9
10
11
12
13
14
15
16
17
18
19
20
21
22
23
24
25
26
27
28
29
30
31
32
33
34
35
36
37
38
39
40
41
42
43
44
45
46
47
48
49
50
51
52
53
54
55
56
57
58
59
60

References

Adams HD, Zeppel MJB, Anderegg WRL, Hartmann H, Landhäusser SM, Tissue DT, Huxman TE, Hudson PJ, Franz TE, Allen CD, Anderegg LDL, Barron-Gafford GA, Beerling DJ, Breshears DD, Brodribb TJ, Bugmann H, Cobb RC, Collins AD, Dickman LT, Duan H, Ewers BE, Galiano L, Galvez DA, Garcia-Forner N, Gaylord ML, Germino MJ, Gessler A, Hacke UG, Hakamada R, Hector A, Jenkins MW, Kane JM, Kolb TE, Law DJ, Lewis JD, Limousin JM, Love DM, Macalady AK, Martínez-Vilalta J, Mencuccini M, Mitchell PJ, Muss JD, O’Brien MJ, O’Grady AP, Pangle RE, Pinkard EA, Piper FI, Plaut JA, Pockman WT, Quirk J, Reinhardt K, Ripullone F, Ryan MG, Sala A, Sevanto S, Sperry JS, Vargas R, Vennetier M, Way DA, Xu C, Yepez EA, McDowell NG (2017) A multi-species synthesis of physiological mechanisms in drought-induced tree mortality. *Nat Ecol Evol* 1:1285–1291. <http://dx.doi.org/10.1038/s41559-017-0248-x>

Allen CD, Macalady AK, Chenchouni H, Bachelet D, McDowell N, Vennetier M, Kitzberger T, Rigling A, Breshears DD, Hogg EH (Ted., Gonzalez P, Fensham R, Zhang Z, Castro J, Demidova N, Lim JH, Allard G, Running SW, Semerci A, Cobb N (2010) A global overview of drought and heat-induced tree mortality reveals emerging climate change risks for forests. *For Ecol Manage* 259:660–684.

Barigah TS, Charrier O, Douris M, Bonhomme M, Herbette S, Améglio T, Fichot R, Brignolas F, Cochard H (2013) Water stress-induced xylem hydraulic failure is a causal factor of tree mortality in beech and poplar. *Ann Bot* 112:1431–1437.

Barrs H., Weatherley PE (1962) A Re-Examination of the Relative Turgidity Techniques for Estimating Water Deficits in Leaves. *Aust J Biol Sci* 15:413–428.

Bartlett MK, Scaffoni C, Sack L (2012) The determinants of leaf turgor loss point and prediction of drought tolerance of species and biomes : a global meta-analysis. *Ecol Lett* 15:393–405.

Berry JA, Beerling DJ, Franks PJ (2010) Stomata: Key players in the earth system, past and present. *Curr Opin Plant Biol* 13:233–240. <http://dx.doi.org/10.1016/j.pbi.2010.04.013>

Bolte A, Czajkowski T, Coccozza C, Tognetti R, De Miguel M, Pšidová E, Ditmarová L, Dinca L, Delzon S, Cochard H, Ræbild A, De Luis M, Cvjetkovic B, Heiri C, Müller J (2016) Desiccation and mortality dynamics in seedlings of different European beech (*Fagus sylvatica* L.) populations under extreme drought conditions. *Front Plant Sci* 7:1–12.

Brodribb TJ, Bowman DJMS, Nichols S, Delzon S, Burlett R (2010) Xylem function and growth rate interact to determine recovery rates after exposure to extreme water deficit. *New Phytol* 188:533–542.

Brodribb TJ, Carriqui M, Delzon S, Lucani C (2017) Optical Measurement of Stem Xylem

- 438 Vulnerability. *Plant Physiol* 174:2054–2061.
- 439 Brodribb TJ, Cochard H (2009) Hydraulic Failure Defines the Recovery and Point of Death in Water-
 440 Stressed Conifers. *Plant Physiol* 149:575–584.
 441 <http://www.plantphysiol.org/cgi/doi/10.1104/pp.108.129783>
- 442 Brodribb TJ, Skelton RP, Mcadam SAM, Bienaimé D, Lucani CJ, Marmottant P (2016) Visual
 443 quantification of embolism reveals leaf vulnerability to hydraulic failure. *New Phytol* 209:1403–
 444 1409.
- 445 Buckley T (2005) The control of stomata by water balance. *New Phytol*:275–292.
- 446 Chaturvedi AK, Patel MK, Mishra A, Tiwari V, Jha B (2014) The SbMT-2 Gene from a Halophyte
 447 Confers Abiotic Stress Tolerance and Modulates ROS Scavenging in Transgenic Tobacco. 9
- 448 Choat B, Badel E, Burlett R, Delzon S, Cochard H, Jansen S (2016) Noninvasive Measurement of
 449 Vulnerability to Drought-Induced Embolism by X-Ray Microtomography. *Plant Physiol* 170:273–
 450 282. <http://www.plantphysiol.org/lookup/doi/10.1104/pp.15.00732>
- 451 Choat B, Brodribb TJ, Brodersen CR, Duursma RA, López R, Medlyn BE (2018) Triggers of tree
 452 mortality under drought. *Nature* 558:531–539. <https://doi.org/10.1038/s41586-018-0240-x>
- 453 Choat B, Jansen S, Brodribb TJ, Cochard H, Delzon S, Bhaskar R, Bucci SJ, Feild TS, Gleason SM,
 454 Hacke UG, Jacobsen AL, Lens F, Maherali H, Martínez-Vilalta J, Mayr S, Mencuccini M, Mitchell
 455 PJ, Nardini A, Pittermann J, Pratt RB, Sperry JS, Westoby M, Wright IJ, Zanne AE (2012) Global
 456 convergence in the vulnerability of forests to drought. *Nature* 491:752–755.
- 457 Cochard H (1992) Vulnerability of several conifers to air embolism. *Tree Physiol* 11:73–83.
- 458 Cochard H (2002) A technique for measuring xylem hydraulic conductance under high negative
 459 pressures. *Plant, Cell Environ* 25:815–819.
- 460 Cochard H, Badel E, Herbette S, Delzon S, Choat B, Jansen S (2013) Methods for measuring plant
 461 vulnerability to cavitation: A critical review. *J Exp Bot* 64:4779–4791.
- 462 Cochard H, Delzon S, Badel E (2015) X-ray microtomography (micro-CT): A reference technology for
 463 high-resolution quantification of xylem embolism in trees. *Plant, Cell Environ* 38:201–206.
- 464 Cochard H, Herbette S, Hernández E, Hölttä T, Mencuccini M (2009) The effects of sap ionic
 465 composition on xylem vulnerability to cavitation. *J Exp Bot* 61:275–285.
- 466 Creek D, Lamarque LJ, Torres-Ruiz JM, Parise C, Burlett R, Tissue DT, Delzon S (2020) Xylem
 467 embolism in leaves does not occur with open stomata: evidence from direct observations using the
 468 optical visualization technique. *J Exp Bot* 71:1151–1159.

- 469 Delzon S, Cochard H (2014) Recent advances in tree hydraulics highlight the ecological significance of
470 the hydraulic safety margin. *New Phytol* 203:355–358.
- 471 Delzon S, Douthe C, Sala A, Cochard H (2010) Mechanism of water-stress induced cavitation in
472 conifers: Bordered pit structure and function support the hypothesis of seal capillary-seeding.
473 *Plant, Cell Environ* 33:2101–2111.
- 474 Duan H, Duursma RA, Huang G, Smith RA, Choat B, O'Grady AP, Tissue DT (2014) Elevated [CO₂]
475 does not ameliorate the negative effects of elevated temperature on drought-induced mortality in
476 *Eucalyptus radiata* seedlings. *Plant, Cell Environ* 37:1598–1613.
- 477 Epila J, De Baerdemaeker NJF, Vergeynst LL, Maes WH, Beeckman H, Steppe K (2017) Capacitive
478 water release and internal leaf water relocation delay drought-induced cavitation in African
479 *Maesopsis eminii*. *Tree Physiol* 37:481–490.
- 480 FAO (2006) Global forest resources assessment 2005—progress towards sustainable forest
481 management. FAO For Pap 147
- 482 Guadagno CR, Ewers BE, Speckman HN, Aston TL, Huhn BJ, DeVore SB, Ladwig JT, Strawn RN,
483 Weinig C (2017) Dead or alive? Using membrane failure and chlorophyll fluorescence to predict
484 mortality from drought. *Plant Physiol* 175:pp.00581.2016.
485 <http://www.plantphysiol.org/lookup/doi/10.1104/pp.16.00581>
- 486 Hacke UG, Venturas MD, Mackinnon ED, Jacobsen AL, Sperry JS, Pratt RB (2015) The standard
487 centrifuge method accurately measures vulnerability curves of long-vesselled olive stems. *New*
488 *Phytol* 205:116–127.
- 489 Hammond WM, Yu KL, Wilson LA, Will RE, Anderegg WRL, Adams HD (2019) Dead or dying?
490 Quantifying the point of no return from hydraulic failure in drought-induced tree mortality. *New*
491 *Phytol:nph.15922*. <https://onlinelibrary.wiley.com/doi/abs/10.1111/nph.15922>
- 492 Hogg EH, Hurdle PA (1997) Sap flow in trembling aspen implications for stomatal responses to VPD.
493 *Tree Physiol* 17:501–509.
- 494 Holbrook NM (1995) Stem Water Storage. *Plant Stems*:151–174.
- 495 Hosking GP, Hutcheson JA (1988) Mountain beech (*Nothofagus solandri* var. *cliffortioides*) decline in
496 the kaweka range, north island, new zealand. *New Zeal J Bot* 26:393–400.
- 497 Intergovernmental Panel on Climate Change (2014) Climate Change 2014: Synthesis Report; Chapter
498 Observed Changes and their Causes.
- 499 Keenan TF, Hollinger DY, Bohrer G, Dragoni D, Munger JW, Schmid HP, Richardson AD (2013)
500 Increase in forest water-use efficiency as atmospheric carbon dioxide concentrations rise. *Nature*

- 501 499:324–327.
- 502 King M., Ludford PM (1983) Chilling injury and electrolyte leakage in fruit of different tomato cultivars.
503 J Am Soc Hort Sci 108:74–77.
- 504 Klimešová J, Nobis MP, Herben T (2015) Senescence, ageing and death of the whole plant:
505 Morphological prerequisites and constraints of plant immortality. New Phytol 206:14–18.
- 506 Körner C (2019) No need for pipes when the well is dry - a comment on hydraulic failure in trees. Tree
507 Physiol. [https://academic.oup.com/treephys/advance-](https://academic.oup.com/treephys/advance-article/doi/10.1093/treephys/tpz030/5425286)
508 [article/doi/10.1093/treephys/tpz030/5425286](https://academic.oup.com/treephys/tpz030/5425286)
- 509 Lamacque L, Charrier G, dos Santos Farnese F, Lemaire B, Ameglio T, Herbette S (2020) Drought-
510 induced mortality: branch diameter variation reveals a point of no recovery in lavender species.
511 Plant Physiol:pp.00165.2020.
- 512 Landmann G, Dreyer E (2006) Impacts of drought and heat on forest. Synthesis of available knowledge,
513 with emphasis on the 2003 event in Europe. Ann For Sci 3 6:567–652.
- 514 Lwanga JS (2003) Localized tree mortality following the drought of 1999 at Ngogo, Kibale National
515 Park, Uganda. Afr J Ecol 41:194–196.
- 516 Martin-StPaul N, Delzon S, Cochard H (2017) Plant resistance to drought depends on timely stomatal
517 closure. Ecol Lett 20:1437–1447.
- 518 Martinez-Vilalta J, Anderegg WRL, Sapes G, Sala A (2019) Greater focus on water pools may improve
519 our ability to understand and anticipate drought-induced mortality in plants. New Phytol
- 520 McDowell N, Pockman WT, Allen CD, Breashears DD, Cobb N, Kolb T, Plaut J, Sperry J, West A,
521 Williams DG, Yezzer EA (2008) Mechanisms of plants survival and mortality during drought: why
522 do some plants survive while others succumb to drought? New Phytol 178:719–739.
- 523 Pammenter N., Vander Willigen C (1998) A mathematical and statistical analysis of the curves
524 illustrating vulnerability of xylem to cavitation. Tree Physiol 18:589–593.
- 525 Petrov V, Hille J, Mueller-Roeber B, Gechev TS (2015) ROS-mediated abiotic stress-induced
526 programmed cell death in plants. Front Plant Sci 6:1–16.
527 <http://journal.frontiersin.org/Article/10.3389/fpls.2015.00069/abstract>
- 528 Reichstein M, Bahn M, Ciais P, Frank D, Mahecha MD, Seneviratne SI, Zscheischler J, Beer C,
529 Buchmann N, Frank DC, Papale D, Rammig A, Smith P, Thonicke K, Van Der Velde M, Vicca S,
530 Walz A, Wattenbach M (2013) Climate extremes and the carbon cycle. Nature 500:287–295.
531 <http://dx.doi.org/10.1038/nature12350>

- 532 Sakes A, Van Wiel M Der, Henselmans PWJ, Van Leeuwen JL, Dodou D, Breedveld P (2016) Shooting
533 mechanisms in nature: A systematic review. PLoS One 11
- 534 Salmon Y, Torres-Ruiz JM, Poyatos R, Martinez-Vilalta J, Meir P, Cochard H, Mencuccini M (2015)
535 Balancing the risks of hydraulic failure and carbon starvation: A twig scale analysis in declining
536 Scots pine. Plant Cell Environ 38:2575–2588.
- 537 Schindelin J, Arganda-Carreras I, Frise E, Kaynig V, Longair M, Pietzsch T, Preibisch S, Rueden C,
538 Saalfeld S, Schmid B, Tinevez JY, White DJ, Hartenstein V, Eliceiri K, Tomancak P, Cardona A
539 (2012) Fiji: An open-source platform for biological-image analysis. Nat Methods 9:676–682.
- 540 Sperry JS, Love DM (2015) What plant hydraulics can tell us about responses to climate-change
541 droughts. New Phytol 207:14–27.
- 542 Sutinen M-L, Palta JP, Reich PB (1992) Seasonal differences in freezing stress resistance of needles of
543 *Pinus nigra* and *Pinus resinosa*: evaluation of the electrolyte leakage method. Tree Physiol 11:241–
544 254. <https://academic.oup.com/treephys/article-lookup/doi/10.1093/treephys/11.3.241> (1 April
545 2019, date last accessed).
- 546 Suzuki N, Koussevitzky S, Mittler R, Miller G (2012) ROS and redox signalling in the response of
547 plants to abiotic stress. Plant, Cell Environ 35:259–270.
- 548 Taiz L, Zeiger E (2006) Plant Physiology. In: Sinauer Associates I (ed) Fourth Edi.pp 46–47.
- 549 Thomas H (2013) Senescence, ageing and death of the whole plant. :696–711.
- 550 Torres-Ruiz JM, Cochard H, Choat B, Jansen S, López R, Tomášková I, Padilla-Díaz CM, Badel E,
551 Burlett R, King A, Lenoir N, Martin-StPaul NK, Delzon S (2017) Xylem resistance to embolism:
552 presenting a simple diagnostic test for the open vessel artefact. New Phytol 215:489–499.
- 553 Torres-Ruiz JM, Cochard H, Mayr S, Beikircher B, Diaz-Espejo A, Rodriguez-Dominguez CM, Badel
554 E, Fernández JE (2014) Vulnerability to cavitation in *Olea europaea* current-year shoots: Further
555 evidence of an open-vessel artifact associated with centrifuge and air-injection techniques. Physiol
556 Plant 152:465–474.
- 557 Torres-Ruiz JM, Jansen S, Choat B, McElrone AJ, Cochard H, Brodribb TJ, Badel E, Burlett R, Bouche
558 PS, Brodersen CR, Li S, Morris H, Delzon S (2015) Direct X-Ray Microtomography Observation
559 Confirms the Induction of Embolism upon Xylem Cutting under Tension. Plant Physiol 167:40–
560 43. <http://www.plantphysiol.org/lookup/doi/10.1104/pp.114.249706>
- 561 Trueba S, Pan R, Scoffoni C, John GP, Davis SD, Sack L (2019) Thresholds for leaf damage due to
562 dehydration: declines of hydraulic function, stomatal conductance and cellular integrity precede
563 those for photochemistry. New Phytol 223:134–149.

- Trumbore S, Brando P, Hartmann H (2015) Forest health and global change. *Science* (80-) 349:814–818.
- Tyree MT, Zimmermann MH (2002) *Xylem structure and the ascent of sap*. Springer, New York, NY.
- Urli M, Porté AJ, Cochard H, Guengant Y, Burlett R, Delzon S (2013) Xylem embolism threshold for catastrophic hydraulic failure in angiosperm trees. *Tree Physiol* 33:672–683.
- Vandegheuchte MW, Guyot A, Hubau M, De Groote SRE, De Baerdemaeker NJF, Hayes M, Welte N, Lovelock CE, Lockington DA, Steppe K (2014) Long-term versus daily stem diameter variation in co-occurring mangrove species: Environmental versus ecophysiological drivers. *Agric For Meteorol* 192–193:51–58. <http://dx.doi.org/10.1016/j.agrformet.2014.03.002>
- Vilagrosa A, Bellot J, Vallejo VR, Gil-Pelegrín E (2003) Cavitation, stomatal conductance, and leaf dieback in seedlings of two co-occurring Mediterranean shrubs during an intense drought. *J Exp Bot* 54:2015–2024.
- Vilagrosa A, Morales F, Abadía A, Bellot J, Cochard H, Gil-Pelegrín E (2010) Are symplast tolerance to intense drought conditions and xylem vulnerability to cavitation coordinated? An integrated analysis of photosynthetic, hydraulic and leaf level processes in two Mediterranean drought-resistant species. *Environ Exp Bot* 69:233–242. <http://dx.doi.org/10.1016/j.envexpbot.2010.04.013>
- Wang C-R, Yang A-F, Yue G-D, Gao Q, Yin H-Y, Zhang J-R (2008) Enhanced expression of phospholipase C 1 (ZmPLC1) improves drought tolerance in transgenic maize. *Planta* 227:1127–1140.
- Wang M, Zheng Q, Shen Q, Guo S (2013) The critical role of potassium in plant stress response. *Int J Mol Sci* 14:7370–7390.
- Widholm J (1972) The use of FDA and phenosafranine for determining viability of cultured plant cells. *Stain Technol* 47:189–94.
- Zhang MIN, Willison JHM (1987) An improved conductivity method for the measurement of frost hardiness. *Can J Bot* 65:710–715. <http://www.nrcresearchpress.com/doi/10.1139/b87-095> (1 April 2019, date last accessed).

Supporting information

Additional supporting information may be found online in the Supporting Information section at the end of the article:

Table S1. PLC evolution during the time-course of the experiment.

Table S2. Evolution of the stem relative water content (RWC_{Stem}), leaf relative water content (RWC_{Leaf}) and electrolytes leakage (EL) during the time-course of the experiment

Table S3. Evolution of the percentage of bark living cells (%BLC) during the time-course of the experiment.

Figure S1. Validation of the Ψ_{stem} measurements recorded with psychrometer and compared to the Ψ_{stem} measurements carried out with the Scholander pressure chamber on previously bagged leaves.

Figure S2. Plants flushing new leaves after re-watering.

Figures legends

Figure 1. Vulnerability curves to cavitation for *P. lusitanica* stems and *P. menziesii* stems. Vulnerability curve for *P. lusitanica* stems obtained on four different samples using the optical method (Brodribb et al. 2017). The P_{50} is evaluated at -6.07MPa while the P_{88} is evaluated at -8.94MPa. Vulnerability curve for *P. menziesii* stems obtained on five different samples using the Cavitrone technique developed by Cochard in 2002. The P_{50} is evaluated at -3.73MPa and P_{88} is evaluated at -5.34MPa. Red solid lines represent the P_{50} while red dashed lines represent the confidence interval around P_{50} at 95%. Violet and green rectangles correspond to the water potential values at which *P. lusitanica* and *P. menziesii* were respectively irrigated.

Figure 2. Box plots representing the dispersions of percentage loss of conductance (PLC) values for A *P. lusitanica* and B *P. menziesii* before water stress (control) and before re-watering for recovering (R) and dead (D) trees measured with the Xyl'EM apparatus for *P. lusitanica* and X-ray micro-CT for *P. menziesii*.

Figure 3. Dynamic of the stem diameter (solid line) and evolution of the water potential (points) during the time-course of the experiment. Stem diameter dynamic (in μm) was recorded by Linear Variable Differential Transformer (LVDT) for both species while the water potential was measured punctually using a Scholander pressure chamber for *P. lusitanica* individuals and continuously by psychrometers for *P. menziesii* individuals. The light grey rectangles represent the period where water was withheld to simulate an extreme drought event. The red line indicates the percentage loss of conductance (PLC) value at which the plant was re-watered. Panels A and B show the recovery of individuals after re-watering in terms of stem diameter while panels C and D show dead individuals.

Figure 4. Variation of Stem Relative Water Content (RWC_{Stem}) (panels A and B), Leaf Relative Water Content (RWC_{Leaf}) (panels C and D), stem Electrolyte Leakage (EL) (panels E and F) for *P. lusitanica* and *P. menziesii*. Measurements were performed on all individuals in control conditions (Control) and after the drought event (i.e. before the rehydration of the plants for recovered and dead individuals).

Figure 5. Cross-sections of *P. lusitanica* (A and B) and *P. menziesii* (C and D) stems in control conditions. Cross-sections were stained using fluorescein diacetate (FDA) (60µm thick cross-section – 1% solution) and microphotographs were taken using a bright light (A and C) and an inverted fluorescence microscope (YFP filter; B and D). Living cells (fluorescent spots) are located in the phloem and outer bark for both species.

Figure 6. Percentage of bark living cells (%BLC) stained with FDA in stem cross-sections in *P. lusitanica* (panel A) and *P. menziesii* (panel B). “R” refers to recovering trees and “D” refers to dead trees.

Table S1. Table summarizing the evolution of the PLC during the time-course of the experiment in A *P. lusitanica* and B *P. menziesii*. Control values represent the mean value of the measurements performed before the drought event. BRW represents the measurements performed on the individuals the day of the rehydration.

Table S2. Table summarizing the evolution of the stem relative water content (RWC_{Stem}), leaf relative water content (RWC_{Leaf}) and electrolytes leakage (EL) during the time-course of the experiment in A *P. lusitanica* and B *P. menziesii*. Control values represent the mean value of the measurements performed before the drought event. BRW represents the measurements performed on the individuals the day of the rehydration.

Table S3. Table summarizing the evolution of the percentage of bark living cells (%BLC) during the time-course of the experiment in A *P. lusitanica* and B *P. menziesii*. Control values represent the mean value of the measurements performed before the drought event. BRW represents the measurements performed on the individuals the day of the rehydration.

Figure S1. Validation of the stem water potential (Ψ_{stem}) measurements recorded with psychrometer and compared to the Ψ_{stem} measurements carried out with the Scholander pressure chamber on previously bagged leaves. A for *P. lusitanica* and B for *P. menziesii*.

Figure S2. Photographs of *P. lusitanica* plants flushing new leaves after experimenting a drought event and reaching levels of PLC of 98.6%. A 19 days after re-watering; B 28 days after re-watering.

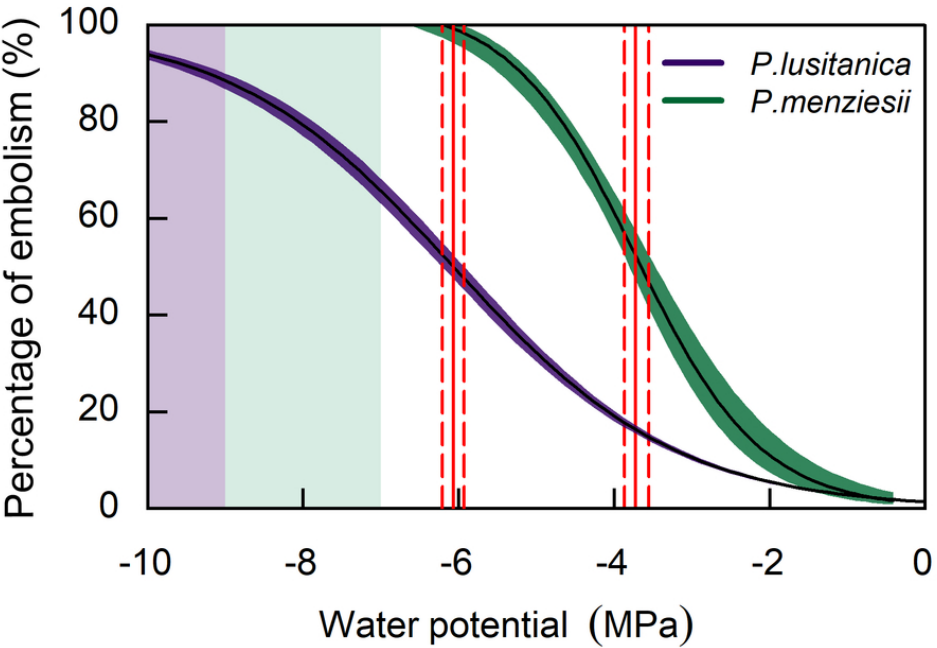
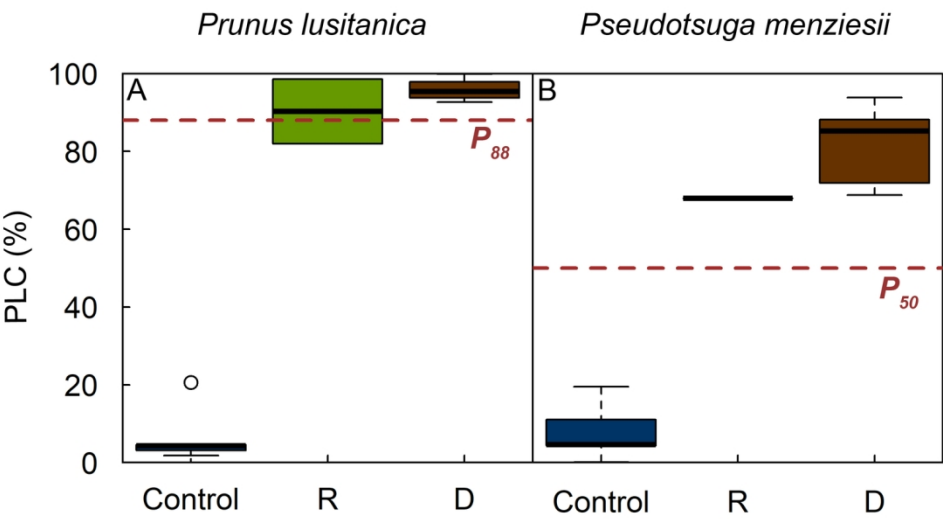


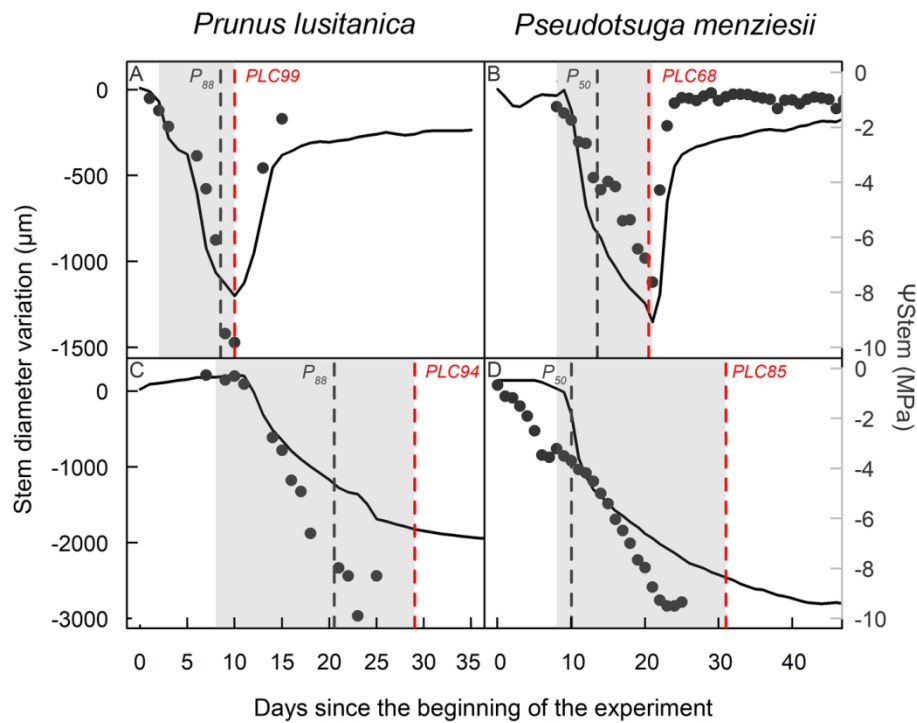
Figure 1. Vulnerability curves to cavitation for *Prunus lusitanica* L stems and *Pseudotsuga menziesii* M stems. Vulnerability curve for *P. lusitanica* stems obtained on four different samples using the optical method (Brodribb *et al.* 2017). The P_{50} is evaluated at -6.07MPa while the P_{88} is evaluated at -8.94MPa. Vulnerability curve for *P. menziesii* stems obtained on five different samples using the Cavitron technique developed by Cochard in 2002. The P_{50} is evaluated at -3.73MPa and P_{88} is evaluated at -5.34MPa. Red solid lines represent the P_{50} while red dashed lines represent the confidence interval around P_{50} at 95%. Violet and green rectangle correspond to the water potential values at which *P. lusitanica* and *P. menziesii* were respectively irrigated.

79x59mm (300 x 300 DPI)



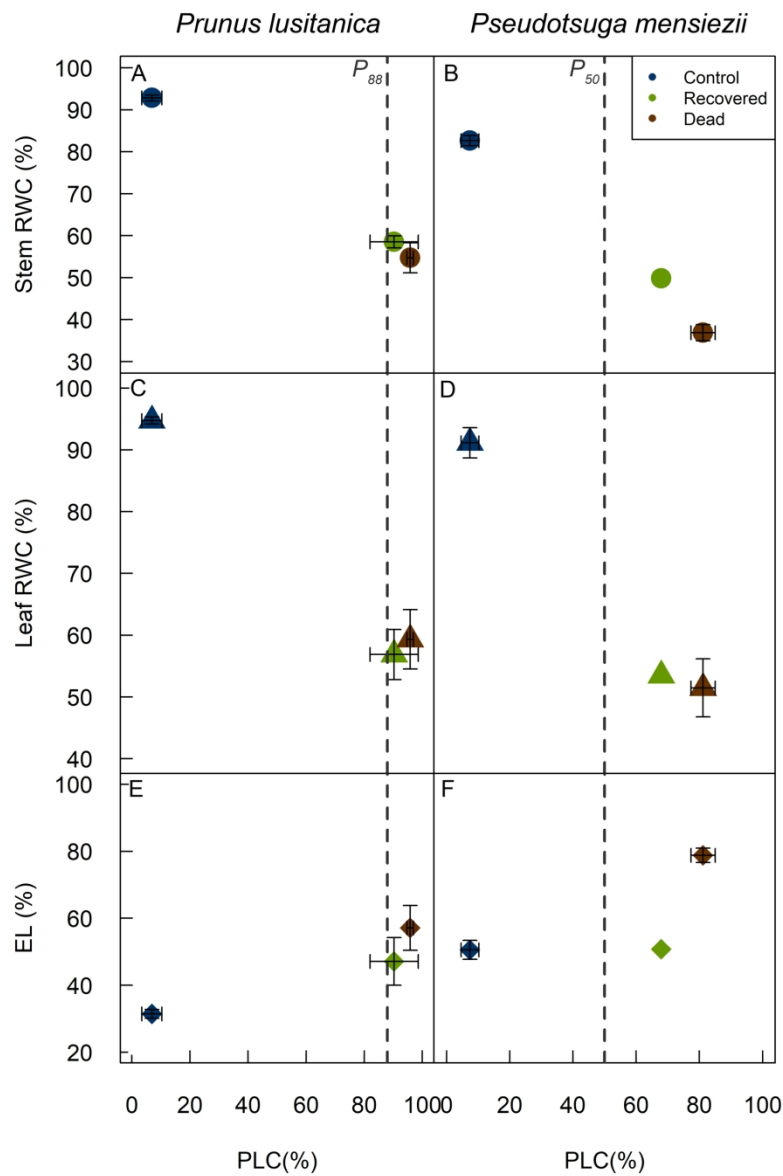
Box plots represents the dispersions of percentage loss of conductance (PLC) values for **A** *Prunus lusitanica*. L and **B** *Pseudotsuga menziesii*. M before water stress (control) and before re-watering for recovering (R) and dead (D) trees measured with the Xyl'ém apparatus for *P. lusitanica* and X-ray micro-CT for *P. menziesii*.

140x79mm (300 x 300 DPI)



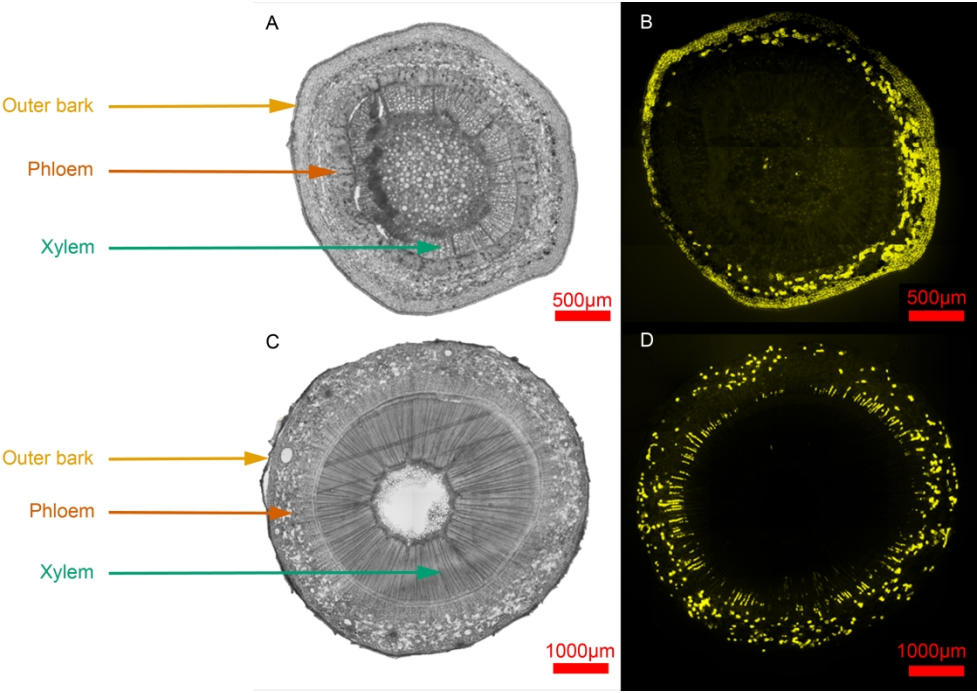
Dynamic of the stem diameter (solid line) and evolution of the water potential (points) during the time-course of the experiment. Stem diameter dynamic (in μm) was recorded by LVDT for both species while the water potential was measured punctually using a Scholander pressure chamber for *Prunus lusitanica* individuals and continuously by psychrometers for *Pseudotsuga menziesii* individuals. The light grey rectangles represent the period where water was withheld to simulate a extreme drought event. Panels **A** and **B** show the recovery of individuals after re-watering in terms of stem diameter while panels **C** and **D** show dead individuals.

132x99mm (300 x 300 DPI)

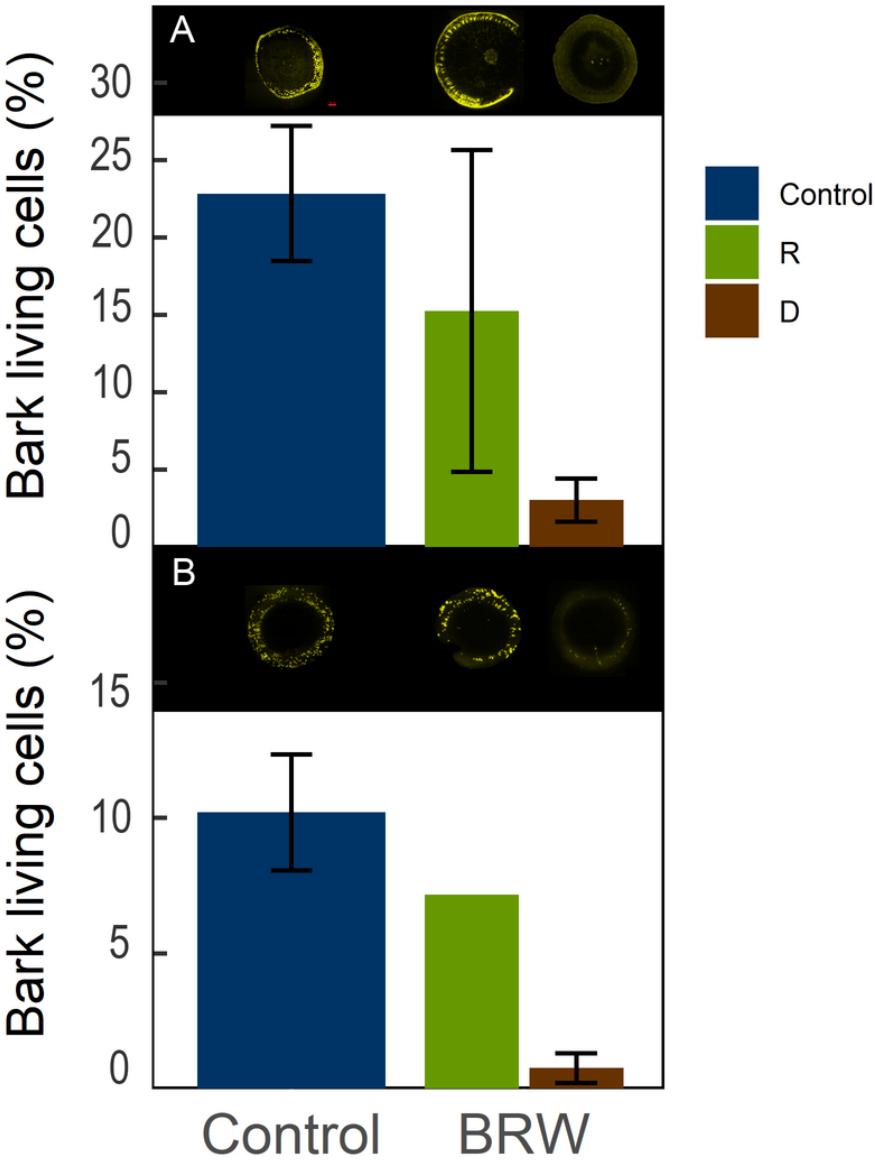


Variation of Stem Relative Water Content (RWC_{Stem}) (panels **A** and **B**), Leaf Relative Water Content (RWC_{Leaf}) (panels **C** and **D**), stem Electrolyte Leakage (EL) (panels **E** and **F**) for *Prunus lusitanica* L and *Pseudotsuga menziesii* M. Measurements were performed on all individuals in control conditions (Control) and after the drought event (e.g. before the rehydration of the plants for recovered and dead individuals).

165x219mm (300 x 300 DPI)



Cross sections of *Prunus lusitanica* L (**A** and **B**) and *Pseudotsuga menziesii* M (**C** and **D**) stems in control conditions. Cross sections were stained using fluorescein diacetate (FDA) (60µm thick cross section – 1% solution) and microphotographs were taken using a bright light (**A** and **C**) and an inverted fluorescence microscope (YFP filter **B** and **D**). Living cells (fluorescent spots) are located in the phloem and outer bark for both species.



Percentage of bark living cells (%BLC) stained with FDA in stem cross section in *Prunus lusitanica* L (panel A) and *Pseudotsuga menziesii* M (panel B). "R" refers to recovering trees and "D" refers to dead trees.

68x90mm (300 x 300 DPI)